The Journal of Immunology

Structure/Function Analysis of Tristetraprolin (TTP): p38 Stress-Activated Protein Kinase and Lipopolysaccharide Stimulation Do Not Alter TTP Function

William F. C. Rigby, Kristen Roy, Jane Collins, Sam Rigby, John E. Connolly, Donald B. Bloch and Seth A. Brooks

J Immunol 2005; 174:7883-7893; ;
doi: 10.4049/jimmunol.174.12.7883
http://www.jimmunol.org/content/174/12/7883

The Journal of Immunology is published twice each month by
The American Association of Immunologists, Inc.,
1451 Rockville Pike, Suite 650, Rockville, MD 20852

Print ISSN: 0022-1767 Online ISSN: 1550-6606.

Structure/Function Analysis of Tristetraprolin (TTP): p38 Stress-Activated Protein Kinase and Lipopolysaccharide Stimulation Do Not Alter TTP Function[1]

William F. C. Rigby,*† Kristen Roy,* Jane Collins,* Sam Rigby,* John E. Connolly,‡ Donald B. Bloch,§ and Seth A. Brooks[2]*†¶

Tristetraprolin (TTP) is the only *trans*-acting factor shown to be capable of regulating AU-rich element-dependent mRNA turnover at the level of the intact animal; however, the mechanism by which TTP mediated RNA instability is unknown. Using an established model system, we performed structure/function analysis with TTP as well as examined the current hypothesis that TTP function is regulated by p38-MAPKAP kinase 2 (MK2) activation. Deletion of either the N- or C-terminal domains inhibited TTP function. Extensive mutagenesis, up to 16%, of serines and threonines, some of which were predicted to mediate proteasomal targeting, did not alter human TTP function. Mutation of the conserved MK2 phosphorylation sites enhanced human TTP function in both resting and p38-stress-activated protein kinase-MK2-activated cells. However, p38-stress-activated protein kinase-MK2 activation did not alter the activity of either wild-type or mutant TTP. TTP localized to the stress granules, with arsenite treatment reducing this localization. In contrast, arsenite treatment enhanced stress granule localization of the MK2 mutant, consistent with the involvement of additional pathways regulating this event. Finally, we determined that, in response to LPS stimulation, human TTP moves onto the polysomes, and this movement occurs in the absence of 14-3-3. Taken together, these data indicate that, although p38 activation alters TTP entry into the stress granule, it does not alter TTP function. Moreover, the interaction of TTP with 14-3-3, which may limit entry into the stress granule, is not involved in the downstream message stabilization events. ***The Journal of Immunology,*** **2005, 174: 7883–7893.**

Regulation of eukaryotic mRNA stability is an important control point in the regulation of gene expression. The AU-rich element (ARE)[3] is a critical *cis*-acting regulatory motif in the 3′-untranslated regions (3′-UTR) of many cytokine and protooncogene mRNAs and a target for *trans*-acting proteins to bind and alter mRNA stability and translation. TNF-α is an inflammatory cytokine expressed by lymphocytes and macrophages and is a critical mediator of inflammation. Activation of macrophages results in a 10,000-fold increase in TNF-α biosynthesis with only a 3-fold increase in transcription (1, 2). Thus, the expression of TNF-α is primarily regulated at the level of mRNA stability and translation (1, 2), with control of both message stability and translation regulated through the TNF-α ARE (2).

The zinc finger protein tristetraprolin (TTP), also known as Nup475, TIS11, G0S24, ZFP36, mediates TNF-α mRNA instability in macrophages (3). Mice that lack TTP spontaneously develop erosive arthritis, cachexia, alopecia, dermatitis, autoantibodies, and myeloid hyperplasia (3). TTP binds directly to the TNF-α mRNA 3′-UTR ARE in vitro (4, 5), establishing TTP as a *trans*-acting factor that binds to the *cis*-acting TNF-α 3′-UTR ARE, increasing the rate of mRNA turnover. Additionally, TTP regulates its expression in a posttranscriptional manner binding to an ARE (defined by nUAUUUAUn sequences) in its own 3′-UTR (6, 7).

Although TTP is a phosphoprotein reported to be a substrate for multiple kinases including ERK, JNK, p38, and MAPKAP kinase 2 (MK2) (8–13), the role of phosphorylation in regulating TTP function is unclear (6–10). Recent work demonstrated that mouse TTP trafficked to the stress granule, an organelle defined by the TIA-1/R proteins (11), which has been implicated in ARE-dependent translational regulation (12). Interestingly, mouse TTP did not traffic to stress granules under arsenite-induced stress due to activation of MK2 by p38 stress-activated protein kinase (SAPK) (13). Mutations of two serines (52/178) in mouse TTP phosphorylated by MK2 (14), resulted in a mouse TTP mutant that still trafficked to the stress granule under conditions of arsenite-induced stress or MK2 activation (13). As part of these studies, it was reported that 14-3-3 interacted with TTP in response to MK2 phosphorylation, suggesting that 14-3-3 interactions prevented TTP entry into the stress granule. Subsequent studies demonstrated that these mutants exhibited enhanced TTP activity on mRNA instability, linking MK2 activation, stress granule entry of TTP, and mRNA turnover (13). 14-3-3 proteins are a family of ubiquitously expressed phosphor-serine, phosphor-threonine binding proteins, which can exert a variety of effects on their binding partner including the following: conformational change; physical occlusion of sequence-specific protein features; and scaffolding functions (15).

Departments of *Medicine, and †Microbiology and Immunology, Dartmouth College, Lebanon, NH 03756; ‡Baylor Institute for Immunology Research, Dallas, TX 75204; §Department of Medicine, Harvard Medical School and the Center for Immunology and Inflammatory Disease of the General Medical Services, Massachusetts General Hospital, Boston, MA 02114; and ¶Veterans Affairs Medical Center, White River Junction, VT 05009

Received for publication February 7, 2005. Accepted for publication April 12, 2005.

The costs of publication of this article were defrayed in part by the payment of page charges. This article must therefore be hereby marked *advertisement* in accordance with 18 U.S.C. Section 1734 solely to indicate this fact.

[1] This work was supported by grants from the Veterans Administration (to S.A.B.), Arthritis Foundation and American Heart Association (to D.B.B.), and AI34928 and AR049834 from the National Institutes of Health (to W.F.C.R.).

[2] Address correspondence and reprint requests to Dr. Seth A. Brooks, Veterans Affairs Medical Center, Research (151), 215 North Main Street, White River Junction, VT 05009. E-mail address: seth.brooks@dartmouth.edu

[3] Abbreviations used in this paper: ARE, AU-rich element; 3′-UTR, 3′-untranslated region; TTP, tristetraprolin; MK2, MAPKAP kinase 2; SAPK, stress-activated protein kinase; DSP, dithiobis-succinimidylpropionate.

0022-1767/05/$02.00

The exact mechanism of cytoplasmic ARE-dependent mRNA turnover remains unclear with various models proposed, including targeting of the mRNA to the 26S proteasome (16), the exosome (17, 18), and the RNA processing body (19, 20). In addition, in vitro data suggested that TTP might contribute to ARE-dependent mRNA deadenylation, although no direct interaction with DAN/PARN was demonstrated (21). Thus, important questions remain regarding the function and regulation of TTP in ARE-dependent turnover.

To begin to address specific mechanisms regulating human TTP function, we examined the role of different TTP protein structural domains, predicted functional domains, and phosphorylation on the ability of TTP to alter TNF-α 3′-UTR-dependent gene expression. Our data indicate that full-length TTP is required to reduce TNF-α 3′-UTR-dependent protein expression, with truncation of the TTP protein resulting in a loss of function. Extensive mutation of serines and threonines (up to 16%) designed to study the role of phosphorylation and targeting to the 26S proteasome had no effect on human TTP function, despite altered mobility of the TTP protein by SDS.

Next, we compared the function of wild-type human and mouse TTP with mutants lacking established (52/178 in mouse) or predicted (60/186 in human) MK2 phosphorylation (13). Mutation of these sites enhanced both human and mouse TTP activity. However, activation of the p38-MK2 pathway either genetically by transfecting constitutively active MEK6 or with LPS stimulation did not result in altered wild-type or MK2 mutant TTP function. As previously reported, mutation of the MK2 sites enhanced stress granule localization of the TTP MK2 mutant under basal conditions (13). However, this localization was further enhanced by arsenite stress. This was in contrast to wild-type TTP, the localization of which decreased with arsenite treatment. Finally, we demonstrated that human TTP localizes to the polysomes in response to LPS stimulation, and this localization occurs in the absence of 14-3-3 interactions. Taken together, these data indicate that 1) p38 activation regulates TTP entry into the stress granule, but does not regulate TTP function; 2) additional pathways regulate TTP entry into the stress granule; and 3) the in vivo interaction of TTP with 14-3-3 does not involve loading of the mRNA onto the polysomes.

Materials and Methods

Reagents

LPS (*Escherichia coli* 026:B6) was purchased from Sigma-Aldrich. Affinity-purified anti-TTP Ab (CARP 3) was generated as previously described (22). Anti-GAPDH Ab (6C5) was purchased from American Research Products. Anti-Xpress Ab (R910) was purchased from Invitrogen Life Technologies. Polyclonal anti-14-3-3 Abs were purchased from Novus Biologicals (Ab-9063) and Santa Cruz Biotechnologies (K19). Monoclonal anti-eIF4E (sc-9976) and goat anti-TIA-1 antiserum (sc-1751) were purchased from Santa Cruz Biotechnologies. Oligonucleotides were purchased from Operon. Dithiobis-succinimidylpropionate (DSP) was purchased from Pierce.

Generation of TTP and luciferase vector constructs

Orientation of the cDNA inserts and the integrity of the DNA sequences were confirmed by sequencing using the ABI Prism Dye Terminator Cycle Sequencing kit (PerkinElmer), and searched against the published sequence (human TTP accession no. M63625, TNF accession no. X01394) on the National Center for Biotechnology Information Database using the BLAST search program (22, 23). The pcDNA 3.1 His-C-TTP (TTP) expression construct (CMV promoter) was generated as previously described (22). The human Delta C truncation was generated by digesting TTP with *Sma*I. TTP PEST mutants were generated by QuikChange mutagenesis (Stratagene). The human TTP serine/threonine point mutants, construct I-XVI, were a generous gift from J. Han (The Scripps Research Institute, La Jolla, CA) (24). Mouse TTP and truncations in Fig. 2 were a generous gift from B. Johnson (Center for Blood Research and Department of Pathology, Harvard Medical School, Boston, MA) (25). All were subcloned into pcDNA 3.1 His-C. The pGL3 luciferase construct (SV40 promoter), contained the human TNF-3′-UTR, nt 855-1643, cloned into the *Xba*I site in the 3′-UTR. Mouse TTP, and TTP-AA in Table III were a generous gift from G. Stoecklin (Division of Rheumatology, Immunology, and Allergy, Brigham and Women's Hospital, Boston, MA) (13). The MEK6DD construct was generous gift from M. Karin (Laboratory of Gene Regulation and Signal Transduction, Department of Pharmacology, University of California San Diego, San Diego, CA) (26).

Transient transfections and luciferase assays

Transient transfections are performed as previously described (6, 22). Briefly, human embryonic kidney (HEK) 293 cells or HEPG2 cells were plated at a density of 300,000 cells per well in six-well plates, with RPMI 1640 supplemented with 10% FCS and 85 ng/ml gentamicin. Each well received the following: 1 μg of pGL3 luciferase vector and varying concentrations of the specified pcDNA 3.1 His C-TTP vector, with the difference in DNA transfected made up with the pcDNA3.1 His-C parental for a total of 1 μg in 100 μl of total, serum free RPMI 1640 medium. The DNA mixture was mixed with 4 μl of Lipofectamine reagent (Invitrogen Life Technologies) in 100 μl of serum-free RPMI 1640, and incubated at 22–25°C for 20 min, following which 800 μl of serum-free medium was added and the mixture was placed over the cells. After 3 h, an equal volume of RPMI 1640 supplemented with 20% FCS medium was added. Transfections for luciferase assays were performed in triplicate in six-well plates and each vector was used in at least three experiments; 293 cells transfected with >90% efficiency. Cells were lysed 24 h after serum addition in 100 μl of 1× lysis buffer, and 20 μl of each sample was read in a luminometer according to the manufacturer's protocol.

For transfection of RAW 264.7 cells, 200,000 cells per well were plated in a 24-well plate and allowed to rest for 48 h. A DNA Lipofectamine mixture was made as outlined above for 293 cells but with the addition of 4 μl of Plus Reagent added to the DNA mixture and the use of 6 μl of Lipofectamine. Each well was washed with serum-free medium and then received the DNA Lipofectamine mixture for 4 h, after which an equal volume of 20% FCS/RPMI 1640 was added. RAW264.7 cell transfection efficiency was >70%.

Real-time PCR

293 cells were lysed in lysis buffer (10 mM Tris (pH 7.5), 150 mM NaCl, 1.5 mM MgCl2, 0.65% Nonidet P-40), vortexed briefly, spun at 12,000 × *g* for 1 min, and the supernatant was collected. Total RNA was isolated from the supernatant using TRIzol (Invitrogen Life Technologies), and the RNA was quantified by spectrophotometry, diluted to 10 ng/μl, and treated with amplification grade DNase (Invitrogen Life Technologies). Reverse transcription was performed using SuperScript II (Invitrogen Life Technologies), 100 ng of mRNA, and oligo(dT) according to the manufacturer's protocol. Following reverse transcription, the reaction was diluted 1/5 with nanopure water.

Real-time PCR was performed as previously described (6). Standard curves were generated from serial dilutions consisting of 10-fold dilutions of a previously amplified copy of the gene being tested (*luciferase*, *actin*) with four points used for each serial dilution. The four dilution points were determined empirically to cover the range of expression of the gene being tested. Standard curves had a correlation coefficient of >0.98 and primer efficiencies were between 97 and 100%. The following primer was used: Luc,sense,GGTGGCTCCCGCTGAATTGG;Luc,antisense,CCGTCATCG TCTTTCCGTG; actin, sense, CAAGCAGGAGTATGACGAGT; and actin, antisense, TGTCAAGAAAGGGTGTAACG.

Sucrose density fractionation

For continuous sucrose gradient fractionation, cells were washed three times with 1× PBS and resuspended in 3.5 ml of buffer A (10 mM Tris-HCl (pH 7.6), 1 mM KAc, 1.5 mM MgAc, 2 mM DTT, 1 mg/ml pepstatin A, 1 mg/ml leupeptin, 1 mM Pefabloc (Roche)) or buffer A containing EDTA (buffer A plus 50 mM EDTA (pH 8.0)). Cells were lysed by 20 strokes with a Teflon pestle homogenizer at 1,500 rpm and centrifuged at 12,000 × *g* for 10 min to pellet the nuclei. Subcellular localization analysis by sucrose density gradient was performed as follows: Postnuclei supernatant was loaded onto the top of 7 ml of a 5–45% continuous sucrose gradient. The samples were centrifuged at 4°C for 5 h at 36,000 rpm. Fractions were collected on a fraction collector in 700-μl aliquots, and the pellet was resuspended in 700 μl.

Immunoblotting

Cytoplasmic preparations were performed as previously described using a method characterized for its lack of contamination by nuclear proteins (22, 27). For immunoblotting, cytoplasmic and gradient fractions were boiled in loading buffer (50 mM Tris-HCl (pH 6.8), 100 mM DTT, 2% SDS, 0.1% bromophenol blue, and 10% glycerol) for 3 min, resolved by 12 or 8–16% SDS-PAGE, and then electrotransferred to nitrocellulose. Immunoblotting was performed with Abs as indicated.

Co(immuno)precipitation

Twenty-four hours after transfection, HEPG2 cells or 293 cells were treated with or without DSP, according to the manufacturer's protocol, and lysed in 400 μl of buffer containing 1% Nonidet P-40, 150 mM NaCl, 50 mM Tris-HCl (pH 8.0), 1 mM MgCl, 10% glycerol, 20 mM 2-ME, 10 mM imidazole, 1 mM Na-vanadate, 50 mM NaF, 20 nM okadaic acid, and EDTA-free complete protease inhibitors (Roche). After incubation for 1 h at 4°C with 40 μl of Ni-NTA magnetic agarose beads (Qiagen), the beads were washed four times in lysis buffer containing 20 mM imidazole and eluted in SDS sample buffer. For coimmunoprecipitation from RAW 264.7 and THP-1 cells, 1.5×10^7 cells were lysed in 150 μl of lysis buffer without 2-ME. Lysates were precleared for 1 h at 4°C with 30 μl of Ultralink beads (Pierce) and incubated for 1–2 h with 2 μg of rabbit anti-TTP (CARP-3) Ab. Ultralink beads (30 ml) were added for 1 h, washed four times in lysis buffer, and eluted at 37°C in SDS sample buffer in the absence of reducing agent.

Immunocytochemistry

HEPG2 cells obtained from American Type Culture Collection and maintained in DMEM supplemented with 10% FCS were grown in tissue culture chambers (Nunc) and transfected with eukaryotic expression vectors encoding wild-type human TTP using the Effectene Transfection System (Qiagen). Twenty-four hours after transfection, cells were exposed to sodium arsenite (0.5 mM; Sigma-Aldrich) for 1 h and were then fixed in 4% paraformaldehyde in PBS, and permeabilized by treatment with methanol. Primary Abs were incubated with fixed cells for 1 h at room temperature, and unbound Abs removed by PBS washes. Goat or rabbit Abs were detected using species-specific, donkey anti-IgG antiserum. Secondary antisera, conjugated with fluorescein or Texas Red (as indicated) were obtained from Jackson ImmunoResearch Laboratories. Cells were stained with 4′,6′-diamidino-2-phenylindole to permit identification of cell nuclei. Cell imaging was performed with a Zeiss Axiophot microscope, and images were processed using Adobe Photoshop 4.0. The association of TTP with stress granules was quantified by scoring HEPG2 cells as positive if wild-type TTP (or Ser→Ala 52/186 TTP) colocalized with TIA-1 at three or more sites within a cell. Three independent transfections were performed, and representative results are presented.

Statistics

An ANOVA was performed for each data set followed by individual comparisons within each data set using Student's *t* test. Stated *p* values are for Student's *t* tests.

Results

Human and mouse TTP behave identically in the model system

Human and mouse TTP, which share ~84% amino acid identity (Fig. 1), were functionally compared in a model using transient transfection of 293 cells (Fig. 2*A*). Equivalent effects and dose responsiveness on human and mouse TNF-α 3′-UTR-dependent luciferase expression were observed, with both human and mouse TTP mediating a significant decrease in TNF-α 3′-UTR-dependent luciferase expression for all concentrations tested ($p < 0.001$). Both human and mouse TTP increased the expression of luciferase from the pGL3 control vector, as previously reported (4, 6, 22). As previously reported, the highest does of TTP mediated a slight increase in TNF-α 3′-UTR-mediated luciferase expression (6, 22). We used the human TTP zinc finger mutant as a negative control; this construct exhibited no inhibitory effect on the human TNF-α 3′-UTR reporter plasmid because it is unable to bind ARE (28). These data indicate that wild-type human and mouse TTP function requires binding of the TNF ARE.

We examined the functional effect of truncating the TTP protein, using previously generated mouse truncation mutants (Fig. 1) (25). Truncation of either the carboxyl or amino ends of mouse TTP resulted in a loss of TTP-mediated inhibition of human TNF-α 3′-UTR-dependent luciferase expression. Both vectors

FIGURE 1. Alignment of human and mouse TTP. Human and mouse truncation mutants are as follows: human Delta C: aa 1–174; mouse N-Zn: aa 1–176; mouse Zn-C: aa 79–319; mouse ZN: aa 79–176. Three human and mouse predicted PEST sequences are indicated in underlined italics. MK2 phosphorylation sites are indicated in bold.

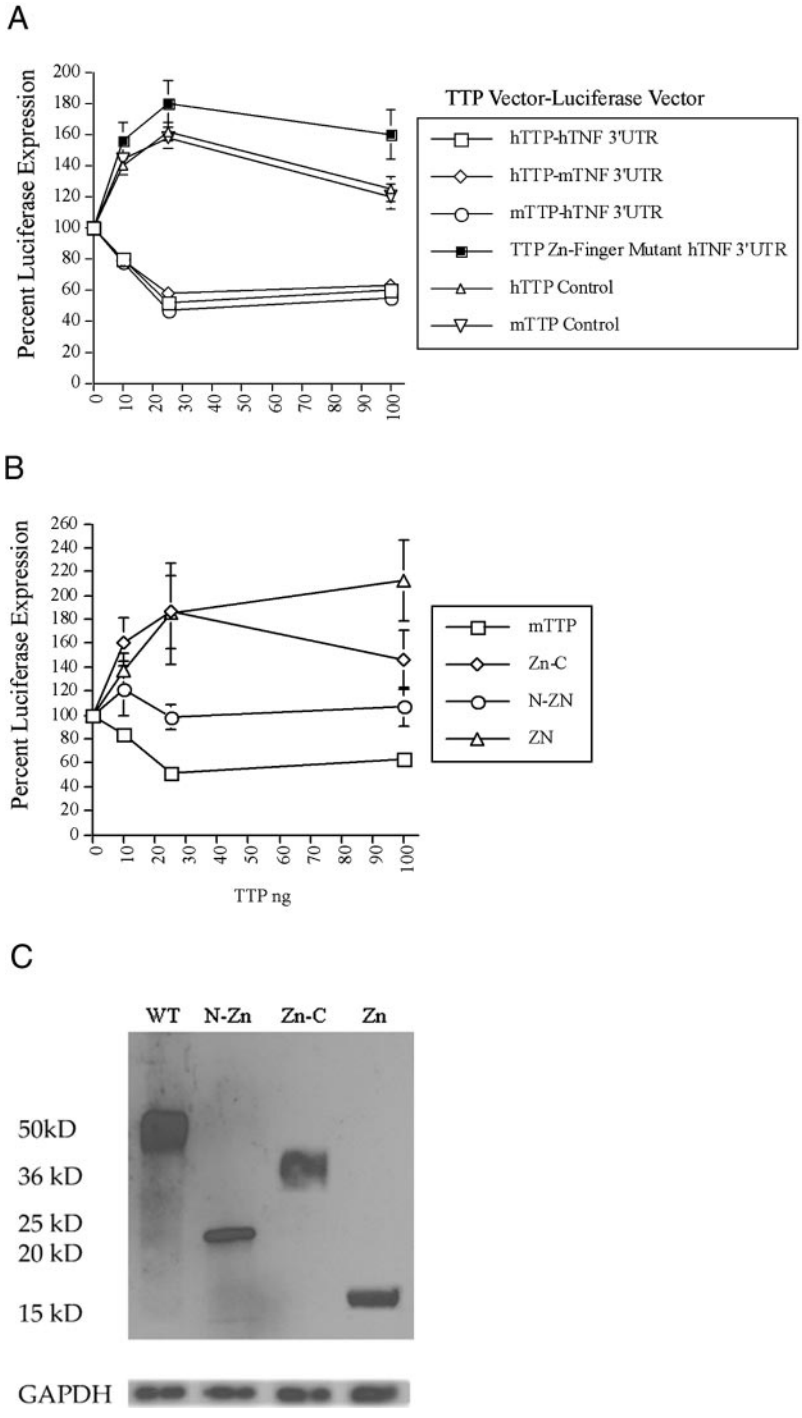

FIGURE 2. Functional comparison of human and mouse TTP on human and mouse TNF-α-dependent reporter gene expression. *A*, 293 cells were transfected with pGL3 luciferase constructs lacking or containing the human or mouse TNF-α 3′-UTR in the absence or presence of the specified amounts of human or mouse TTP cDNA. Luciferase activity is shown as a function of that obtained in the absence of TTP cDNA cotransfection. *B*, Examination of mouse TTP truncation mutants. *C*, Immunoblotting of cytoplasmic lysates from 293 cells transfected with specified mouse TTP constructs. Blotted with anti-Xpress. GAPDH loading control is below (see Table I).

were significantly different ($p < 0.03$) from wild type at all three transfection concentrations (Fig. 2*B*). Similar results were obtained with the human TTP lacking the C terminus (data not shown). Mouse TTP containing only the zinc finger domain (ZN) exhibited no activity. Immunoblotting (Fig. 2*C*) revealed that wild-type and N-terminal deficient (Zn-C) mouse TTP mutant migrated with size heterogeneity as well as significantly larger mass (10–15 kDa) than predicted (Table I). These features are not apparent with mu-

Table I. *List of mouse TTP expression constructs*

Vector	Description	Predicted Molecular Mass (kDa)	pI
TTP-Mouse	Full length-wild-type mouse TTP 1–319	33.6	8.8
Zn-C	aa 79–319, N-terminal truncation	25.5	9.3
N-Zn	aa 1–176, C-terminal truncation	19.2	8.7
Zn	aa 79–176, zinc-finger domain alone	11	9.4

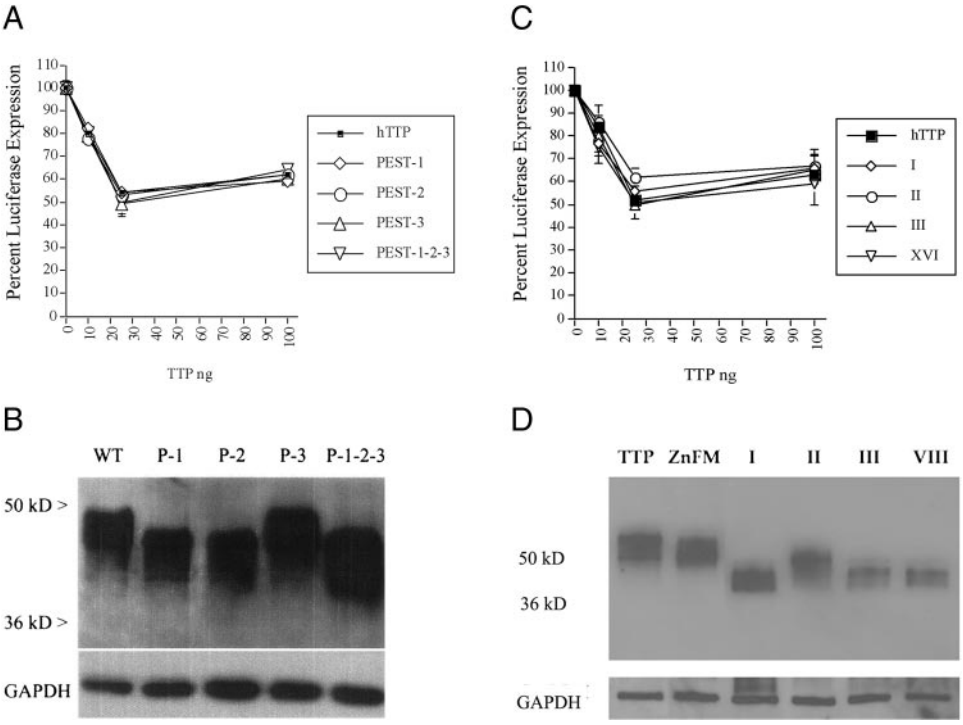

FIGURE 3. Inactivation of predicted PEST domains and sites of phosphorylation fail to alter human TTP function. *A*, PEST-1, PEST-2, PEST-3, and PEST-1-2-3 (see Table II) mutants were compared with wild-type human TTP in their effects on human TNF-α 3′-UTR-dependent luciferase expression in 293 cells, as described in Fig. 2. *B*, Immunoblotting of PEST TTP mutants demonstrating increased mobility of TTP proteins containing the PEST-1 or PEST-2 mutations, and no change in protein levels. *C*, Human TTP mutants I, II, III, and XVI containing cassettes of serine/threonine→alanine mutations (see Table II) were examined for their effects on human TNF-α 3′-UTR-dependent luciferase expression in 293 cells relative to wild-type human TTP. *D*, Immunoblotting of serine/threonine TTP mutants.

tant mouse TTP lacking the C terminus (Zn-C, ZN), suggesting that TTP signal heterogeneity on immunoblotting is mediated through posttranslational modifications of the C terminus.

Identification of predicted TTP functional domains

In light of these data, we screened human TTP for putative functional domains. Three predicted PEST domains, polypeptide sequences enriched in proline (P), glutamic acid (E), serine (S), and threonine (T) that target proteins for rapid destruction, with very high scores (9.95, 11.03, 15.57) were identified using the PEST-FIND program (⟨http://bioweb.pasteur.fr/seqanal/interfacs/pest-find-simple.html⟩). PEST sequences target proteins to the 26S proteasome for degradation. The 26S proteasome also contains RNases and has been suggested by various studies to be a site of ARE-dependent mRNA turnover (16, 29).

Point mutations predicted to abolish the activity of these putative PEST sequences (30, 31) were generated and functionally characterized. The function of TTP was unaffected by any single or combined series of mutations of these sequences (Fig. 3*A*, Table II). Immunoblotting demonstrated equivalent levels of TTP expression (Fig. 3*B*). Thus, although these sequences all had high predicted PEST scores, they do not appear to mediate TTP protein turnover or alter TTP function. Mutation of serines 43 (P-1) and 93 (P-2) in the N terminus altered TTP migration, suggesting their potential identity as sites of phosphorylation, consistent with the identification of mouse serine 85 as an MK2 phosphorylation target in vivo (14).

Effect of phosphorylation on TTP function

To further examine the role of phosphorylation on human TTP function, we used a previously generated set (Table II) of human TTP serine/threonine mutants (24). These mutants (I-XVI) all carry various cassettes of 3–12 serine/threonine→alanine mutations, with 16% of the serine/threonines in TTP mutated in XVI. No obvious difference between wild-type and mutant TTP (Fig. 3*C*) (only mutants I, II, III, and XVI are shown). Immunoblotting demonstrated increased mobility of mutants I, II, and XVI (Fig. 3*D*), suggesting that mutants I and II contain sites of phosphorylation, many of which correspond to sites that are phosphorylated in mouse TTP (14).

MK2 phosphorylation and human TTP function

Chrestensen et al. (14) reported that serines 52 and 178 in mouse TTP were in vivo substrates for MK2, a finding of considerable

Table II. *Human TTP serine/threonine point mutants (I-XVI, S→A)→alanine, PEST serine→arginine*

Mutant	43S	60S	88S	90S	93S	186S	196T	197S	214S	216S	218S	228S	238S	257T	271T	296S
I													+	+	+	+
II			+	+	+											
III								+	+		+	+				
XVI			+	+	+		+	+	+		+	+	+	+	+	+
PEST-1	+															
PEST-2					+											
PEST-3										+						
PEST-1–2	+				+											
PEST-1–2-3	+				+					+						
S→A60		+														
S→A186						+										
S→A60,186		+				+										

interest, because the p38α-MK2 pathway regulates TNF-α mRNA stability and translation (2, 32). Building on prior work (25), MK2 phosphorylation of these sites was reported to enable 14-3-3 binding and limited trafficking of murine TTP to stress granules (13). This latter effect was associated with a decreased ability of TTP to mediate destabilization of a TNF-α ARE-containing construct. Because human TTP contains serines at 60 and 186 in the identical context to serines 52 and 178 in the mouse (Fig. 1), we tested whether these sites function in the same manner in human TTP (Fig. 4*A*). Single (serine→alanine) mutation of serines 60 and 186 did not alter TTP function, whereas the double mutant (S→A 60,186) enhanced function relative to wild-type human TTP ($p < 0.05$ at all three concentrations). Using real-time PCR, we determined that these effects were mediated at the message level, with TTP expression reducing luciferase mRNA accumulation in a manner parallel to that seen with luciferase protein (data not shown).

Cotransfection of constitutively active MEK6 (MEK6DD), (Fig. 4*B*), doubled TNF-α 3′-UTR-dependent luciferase expression ($p < 0.001$), consistent with activation of the p38-MK2 pathway (2, 33). TTP continued to mediate a reduction in TNF-α 3′-UTR specific luciferase expression with MEK6DD cotransfection, and

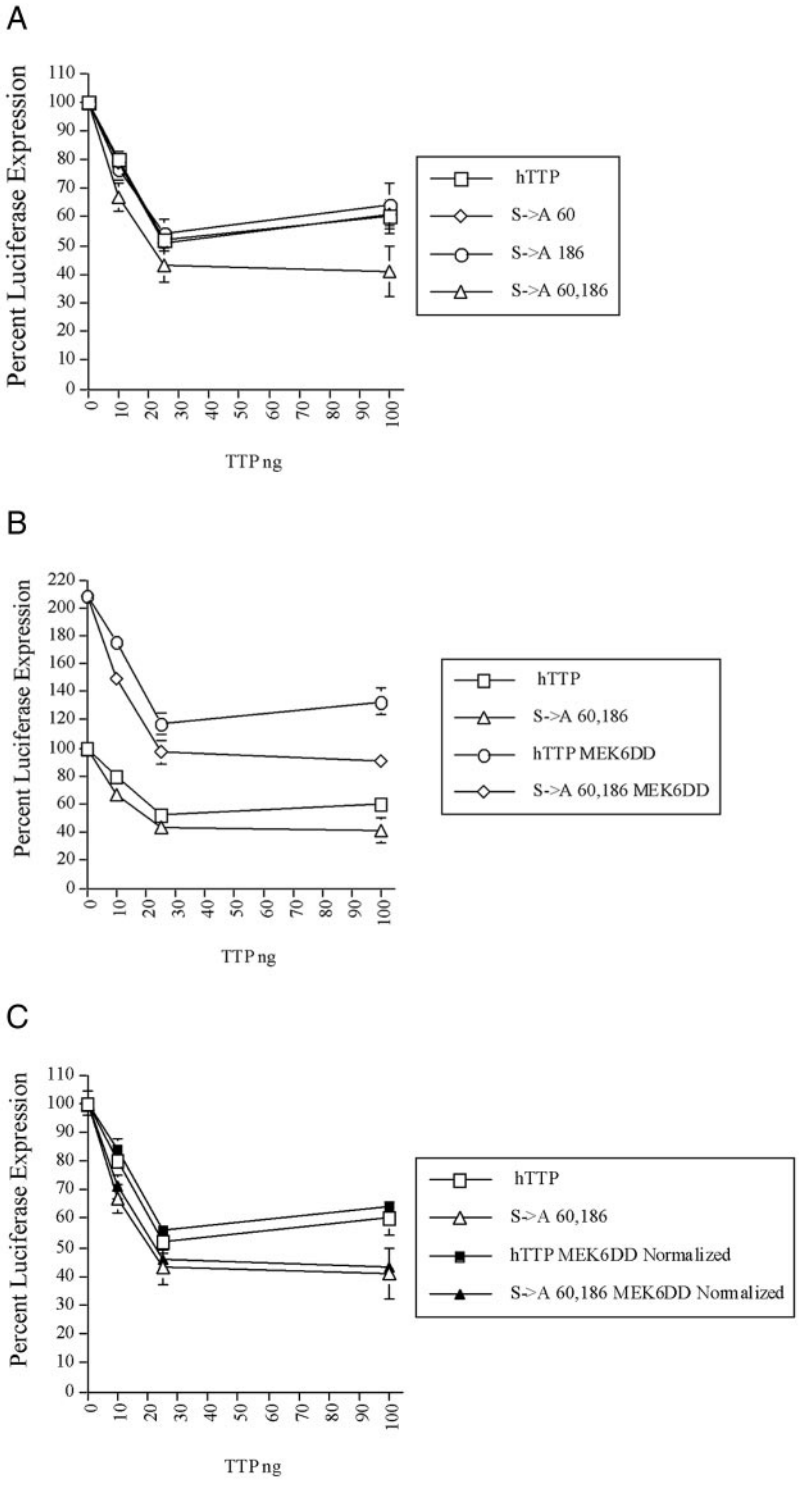

FIGURE 4. Mutation of serines 60 and 186 results in enhanced TTP function. *A*, The effect of mutating serines 60 and 186 individually and together was examined. *B*, Effect of p38 activation on wild-type and mutant TTP function. 293 cells were activated by cotransfecting 100 ng of constitutively active MEK6 vector, MEK6DD. *C*, Normalization of the data graphed in *B* to account for the effect of MEK6DD cotransfection of TNF-α 3′-UTR-mediated luciferase expression.

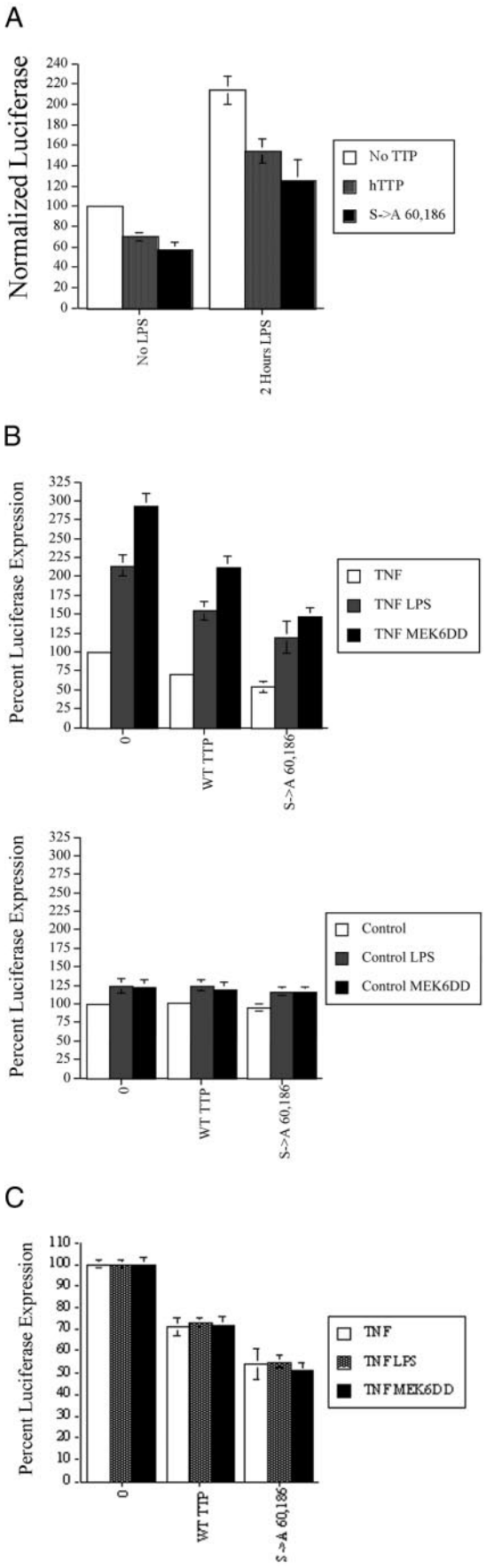

FIGURE 5. Examination of TTP and TNF-α 3′-UTR luciferase expression in resting and activated RAW 264.7 cells. RAW 264.7 cells were transfected with either the control luciferase (pGL3-Control) or human TNF-α 3′-UTR (pGL3-TNF) luciferase vectors and no TTP, or 25 ng of wild-type human TTP or S→A 60,186 MK2 mutant. *A*, Graphing the data as a function of LPS activation (10 ng/ml, 2 h) demonstrates LPS stimulated increases in TNF-α 3′-UTR-mediated luciferase expression. *B*, Activation with either LPS or MEK6DD results in a significant increase in luciferase expression ($p < 0.0001$), with the effect clearly mediated by the TNF-α 3′-UTR. These data are normalized to no TTP, no activation. *C*, Normalization of the data in *B* to the no TTP transfection for each group reveals the effect of TTP cotransfection. In the absence of activation, TTP and S→A 60,186 mediate a significant reduction in luciferase expression ($p < 0.05$), with S→A 60,186 functionally more active than wild-type mTTP, ($p < 0.05$). Activation with MEK6DD or LPS does not alter the percent inhibition mediated by either human TTP or S→A 60,186.

the S→A 60,186 TTP mutant remained more active than wild-type TTP. Normalizing the data to account for the MEK6DD-mediated increase in TNF-α 3′-UTR luciferase expression (Fig. 4*C*) (MEK6DD with TTP/MEK6DD No TTP) demonstrates no change in the function of either wild-type or S→A 60,186 mutant TTP. Thus, activation of the p38-MK2 pathway in 293 cells did not significantly affect the ability of either wild-type or mutant human TTP to regulate TNF-α 3′-UTR-dependent gene expression.

Because our results differed from previous work in RAW 264.7 murine macrophage cells (13), we repeated these studies in this cell line with both human and mouse wild-type and mutant TTP as well as human and mouse TNF-α 3′-UTR luciferase, respectively. When TNF luciferase values are normalized to the value obtained with the control (TNF luciferase/Control luciferase) to account for transcriptional activity, and graphed as a function of LPS activation (Fig. 5*A*), our data give comparable results to those of Stoecklin et al. (13). That being so, LPS stimulation increases TNF-α 3′-UTR expression, TTP reduces this expression, and the TTP-AA mutant (mouse S→A 52,178) mutant is more active. Based on these data, it was concluded that phosphorylation of TTP at serines 52 and 178 was responsible for posttranscriptional induction of TNF-α expression by LPS (13).

Presenting the data in this manner does not examine the effect of LPS activation on TTP function; it only calculates the effect of LPS on TNF-α 3′-UTR-mediated luciferase expression. To determine the effect of LPS stimulation on TTP function, we normalized these data as in Fig. 4 (luciferase expression for condition X/luciferase expression with no TTP and no activation) to yield the fold induction for activation (Fig. 5*B*). This reveals a significant increase in TNF-α 3′-UTR luciferase expression mediated by both LPS and MEK6DD ($p < 0.001$). To determine whether either LPS or MEK6DD activation altered TTP function, we then normalized luciferase expression within each condition (luciferase expression with TTP/luciferase expression with no TTP for each condition) (Fig. 5*C*). Analyzed in this manner, neither LPS activation nor MEK6DD cotransfection alters the function of TTP or the TTP MK2 mutant, which remains more active than wild-type TTP. Similar results were obtained using the mouse constructs (data not shown).

TTP localization to the stress granule

TTP overexpression promotes assembly of stress granules that included TTP, whereas arsenite treatment excludes TTP from stress granules (13). We examined the localization of wild-type and mutant human and mouse TTP by indirect immunofluorescence in the HEPG2 hepatoma cell line (Fig. 6, human TTP; with human and mouse data summarized in Table III). Stress granule localization is indicated by the presence of TIA-1 (13). Under resting conditions, TTP expression induced stress granule formation and localization in a small percentage (5–12%) of cells (Fig. 6, *A–C*; Table III).

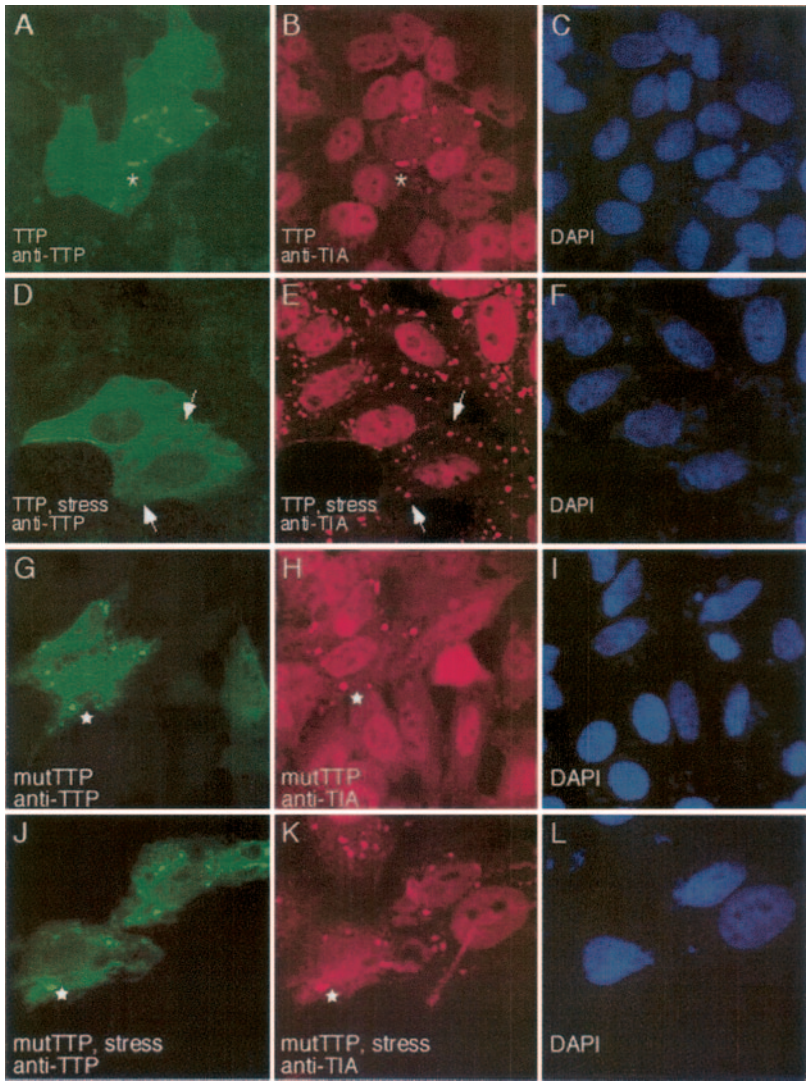

FIGURE 6. Examination of wild-type and mutant, human and mouse TTP localization to stress granules in HEPG2 cells. Following transfection with the indicated TTP construct, HEPG2 cells were cultured in medium alone or containing arsenite (0.5 mM, 60 min). TTP, green; TIA, red; and 4′,6′-diamidino-2-phenylindole (DAPI), blue. TIA indicates location of stress granules. *A–C*, Wild-type human TTP: 12% of transfected cell have TTP in stress granules. *D–F*, Wild-type human TTP plus arsenite: 3% of transfected cell have TTP in stress granules. *G–I*, Mutant human TTP: 21% of transfected cell have TTP in stress granules. *J–L*, Mutant human TTP plus arsenite: 30% of transfected cell have TTP in stress granules. Human and mouse data are summarized in Table III.

Arsenite treatment induced stress granules in nearly all HEPG2 cells, with marked reduction in the percentages of cells that exhibited TTP-positive stress granules (Fig. 6, *D–F*; Table III). Both human (S→A 60,186) and mouse (TTP-AA) mutants colocalized to a much higher percentage of stress granules in resting cells (Fig. 6, *G–I*; Table III), as previously reported (13). Importantly, localization of the TTP MK2 mutant was enhanced by arsenite treatment (Fig. 6, *J–L*), in contrast to wild-type, which decreased with arsenite treatment.

Human TTP loads onto polysomes in response to LPS activation without 14-3-3

Exclusion of TTP from arsenite-induced stress granules was shown to correlate with 14-3-3 interactions (13). Using an identical protocol, we were unable to demonstrate an interaction between TTP and 14-3-3 proteins in Ni-NTA precipitates from 293 and HEPG2 cytosols under basal or p38-MK2 activation conditions. HEPG2 cytosols exhibit much higher levels of 14-3-3 proteins (see "Depleted" fractions, *right panel*, Fig. 7*A*) that were shown to nonspecifically associate with Ni-NTA beads in untransfected (NT) cells, in the absence of TTP expression. Some TTP was shown to interact with 14-3-3 proteins under conditions of MEK6DD expression and activation of p38-MK2 in HEPG2 cells. This interaction was not evident in either HEPG2 or 293 cells with the addition of the cleavable protein cross-linking reagent DSP for the last 15 min before cell lysis. Two interpretations of these data seem possible. First, in cells that express high levels of 14-3-3 proteins, an interaction with overexpressed TTP can be demonstrated under conditions of p38-MK2 activation, but this interaction might occur after cell lysis. Alternatively, 14-3-3 proteins are able to stick to Ni-NTA beads nonspecifically, and this interaction may be enhanced by p38-MK2 activation.

Table III. *TTP stress granule localization in Hen2 cells*

	Wild-Type Human TTP (%)	Wild-Type Mouse TTP (%)	Serine 60,186 Human TTP (%)	Mouse TTP-AA (%)
Resting	12	5	21	28
Arsenite	3	0	30	42

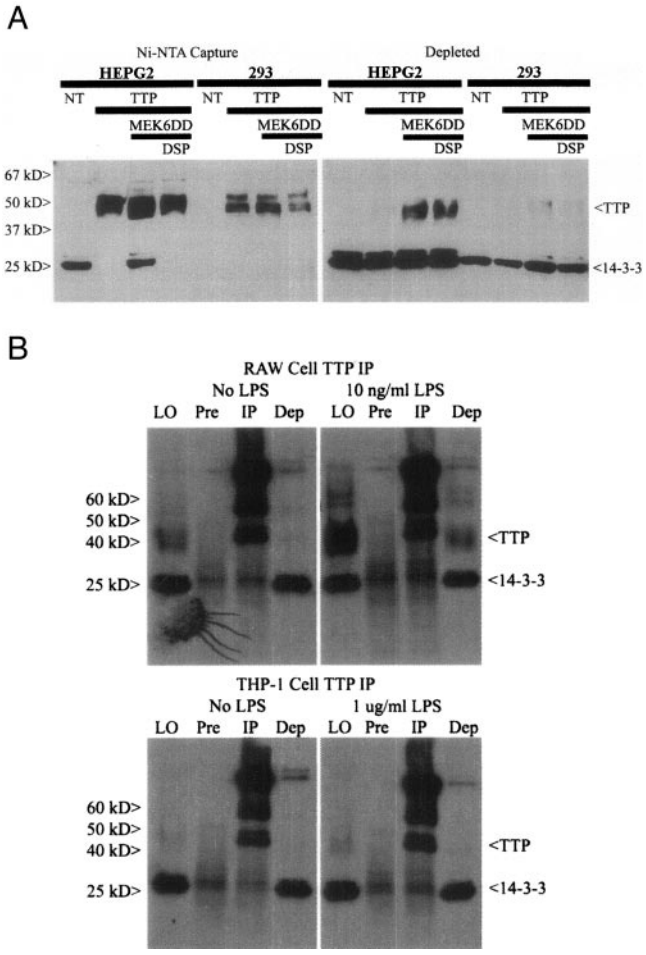

FIGURE 7. 14-3-3 does not coprecipitate with TTP as a function of p38 activation. *A*, Following transient transfection with His-tagged human TTP in the absence or presence of MEK6DD expression. TTP was coprecipitation using Ni-NTA magnetic agarose beads and immunoblotted for TTP and 14-3-3 (13). Nontransfected (NT) cells are used as a control for nonspecific adherence. Depleted lysates represent 6% of the precipitated lysate. DSP was added to a separate set of the MEK6DD transfected cultures 15 min before cell lysis. *B*, TTP was immunoprecipitated from resting or LPS-activated RAW 264.7 cell or THP-1 cell cytosols and blotted for TTP and 14-3-3. LO, Load on, 5% of the lysate used for immunoprecipitation. "Pre" represents the Ultralink protein A/G beads used to preclear the lysate (note 14-3-3, but not TTP in these lanes). Dep, Depleted fraction, 5% of lysate remaining after immunoprecipitation (IP).

Due to these results, we examined the interaction of native human and mouse TTP using immunoprecipitation from the monocyte-macrophage cell lines THP-1 and RAW264.7. LPS treatment increased immunoprecipitable TTP protein levels (Fig. 7*B*). Although 14-3-3 proteins were coprecipitated, this apparent interaction was unaffected by LPS treatment, which induces p38-MK2 activation. Given the enhanced levels of TTP from LPS-treated cells, the demonstration of equivalent levels of 14-3-3 proteins suggests that LPS treatment reduces these interactions. It is noteworthy that the levels of 14-3-3 proteins associated with the beads used to preclear the lysate are equivalent to that seen in the immunoprecipitate, again suggesting a nonspecific interaction as seen in the HEPG2 cytosols with Ni-NTA beads.

One model of TTP function is that 14-3-3 binding to TTP limits TTP entry into the stress granule, preventing TTP from directing its associated mRNA to the degradative machinery. By extension, this suggests that TTP 14-3-3 complexes may be components of

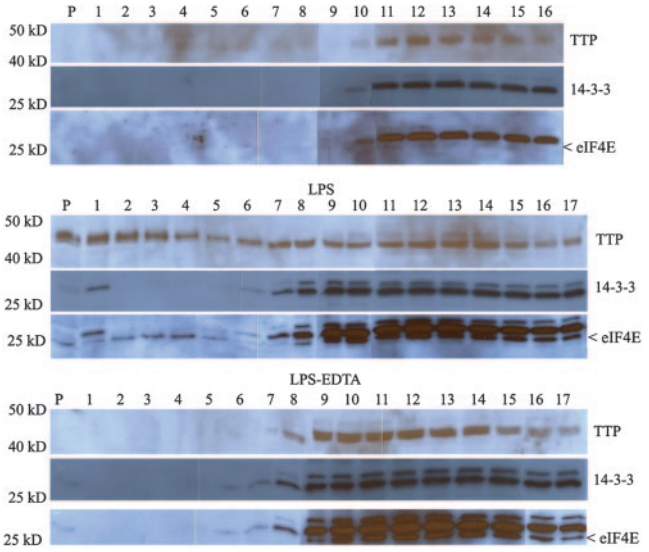

FIGURE 8. TTP moves onto the polysomes following LPS stimulation in THP-1 cells in the absence of 14-3-3 proteins. THP-1 cytoplasmic lysate from unstimulated, LPS-stimulated, and EDTA-treated LPS-stimulated was fractionated on a 5–45% linear sucrose gradient. Twenty-five microliters of each 700-μl fraction was examined by 8–16% SDS-PAGE and blotted for TTP, 14-3-3, and eIF4E. "P" is the pellet, and "1" is the densest fraction.

polysomal mRNA (13). To test this hypothesis, we examined the localization of TTP and 14-3-3 by continuous sucrose density fractionation (5–45%) in resting and LPS-activated THP-1 cells. TTP and 14-3-3 were primarily located in the less dense fractions in resting cells (Fig. 8). LPS activation (1 μg/ml; 2 h) increased TTP expression as previously reported (6), as well as induced distribution into denser fractions with the initiation factor eIF4E, but with little or no 14-3-3 proteins (Fig. 8). The presence of EDTA, which disrupts polyribosomes (34), results in a loss of TTP and eIF4E localization to these dense fractions, confirming the polysomal localization of TTP (Fig. 8). Thus, little if any TTP-14-3-3 interaction occurs on the polysomes.

Discussion

Although TTP is one of the best-characterized ARE binding proteins, its specific mechanism of action in mediating mRNA decay has not been established. Using HEK 293 cells, which express little or no native TTP, we examined the structure-function relationship of TTP in mediating mRNA instability. We determined that both the N- and C-terminal domains were necessary for function. Mutations of predicted PEST sequences and 12 potential phosphorylation sites did not alter TTP levels or function, leading us to conclude that these subdomains or sites are not critical in regulating TTP function with regard to TNF-α mRNA stability. Interestingly, several of the mutations increased TTP mobility by SDS-PAGE, consistent with phosphorylation at these sites (Fig. 3). Although mutagenesis studies reveal a robust TTP phenotype in terms of regulating TNF-α 3′-UTR expression, there is a requirement for the N- and C-terminal domains for TTP function. Indeed, recent work indicates that a number of RNA degradative enzymes associated with the N terminus of TTP, but optimal destabilizing activity required both the N-terminal and C-terminal domains (35).

TTP trafficking to the stress granule and the role of phosphorylation

We examined the model in which TTP entry into the stress granule is regulated by MK2-mediated phosphorylation (13). In this

model, phosphorylation of serines 52 and 178 enabled 14-3-3 binding, preventing stress granule entry of TTP resulting in the stabilization of the TNF-α message (13). Our findings are consistent with some aspects of this model (13). We find that expression of transfected TTP resulted in spontaneous stress granule formation and localization of TTP to these structures. Similarly, arsenite treatment reduced the stress granule localization of TTP. We also observed that mutation of the serines (52/178 in the mouse, 60/186 in the human) increased TTP localization to stress granule under resting conditions. Expanding on this previous work, our studies demonstrate that the TTP MK2 mutants exhibit increased stress granule localization under arsenite stress. This finding is notable, because it indicates an additional pathway(s) that is triggered by cellular stress, which positively regulates TTP entry into the stress granule. In the absence of MK2-dependent phosphorylation, the effects of this alternative pathway become more evident.

TTP does not interact with 14-3-3 proteins on the polysomes

We examined the possible role of 14-3-3 proteins in regulating TTP function. We observed that TTP moves onto the polysomes following LPS activation, and this occurs independent of 14-3-3 proteins. Moreover, we failed to demonstrate a specific interaction of either native or transfected human or murine TTP with 14-3-3 proteins under basal or activated conditions, using an identical protocol and reagents (13). Attempts to stabilize weak interactions between TTP and 14-3-3 proteins using protein-protein cross-linking reagents before cell lysis did not alter this result. We cannot explain these differing results, because the TTP-14-3-3 interaction has been reported by Ab supershifting of radiolabeled TNF-α RNA, yeast two-hybrid screening as well as with recombinant proteins (13, 25). Our data suggest the possibility that TTP-14-3-3 complexes may form during or after cell lysis. Alternatively, the TTP-14-3-3 interaction may occur with only a small fraction of the cytosolic TTP pool; if that is true, it is hard to account for its functional importance. We are exploring alternate strategies to confirm this interaction. Currently, we conclude that if 14-3-3 interactions alter the entry of TTP into the stress granule entry (13), polysomal loading appears to necessitate dissociation of 14-3-3 from TTP.

Regulation of TTP function by the p38-MK2 pathway

Activation of the p38-MK2 pathway increased TNF-α 3′-UTR-mediated luciferase expression. There was no difference in the magnitude of this effect when examined as a function of TTP expression (Figs. 4 and 5). These data are consistent with that of other investigators indicating a lack of a relationship between TTP function and the p38-MK2 pathway. Pharmacologic inhibition of p38 SAPK still reduces TNF-α biosynthesis in TTP-deficient mouse macrophages (33). In addition, splenocytes from MK2-deficient mice exhibit decreased TNF-α production (36, 37), but with normal levels of mRNA, suggesting a role in translation, not mRNA turnover, as one would expect with changes in TTP function (4, 36, 37). Finally, phosphorylation on serines 52/178 has not been correlated with changes in TTP function (7). Thus, there are extensive data in the literature implying a lack of effect of MK2 activation on TTP function (4, 7, 33, 36, 37); our data now demonstrate this explicitly.

Mutation of the MK2 phosphorylation sites enhanced both human and mouse TTP function and stress granule localization. Thus, our findings are consistent with the model that the stress granule, an organelle important in translational regulation (11, 12), is linked to subsequent TTP-mediated mRNA decay. Our findings suggest that MK2 activation negatively influences TTP entry into the stress granule, but that additional events or signaling pathways may regulate entry of the TTP-mRNA particle into the stress granule as well as its subsequent transition to a site of mRNA decay. In this regard, recent studies indicate that stress granule entry and function of a TTP homolog, BRF1, are coordinately regulated by protein kinase B-dependent serine phosphorylation (38).

Previously, we showed that TTP interacts with its target mRNA under resting and activated conditions (6), apparently binding its mRNA ligand in a constitutive manner. The Blackshear laboratory (8) has reported that the phosphorylation status of TTP does not impact its binding to the TNF-α mRNA. Our data support the hypothesis that TTP remains bound to its mRNA ligand following LPS stimulation and moves with that ligand onto the polysomes. In this model, TTP binds specific AREs in a constitutive manner, whereas the functional consequences of this interaction (rates of mRNA deadenylation or degradation) are determined by its interaction with other proteins (21), which are the targets of specific signaling cascades. Illustrating this is the observation that TTP mRNA stability is differentially regulated over time by the ERK MAPK and p38 SAPK pathways following LPS activation (6, 7). We are currently pursuing a strategy of identifying the proteins that interact with TTP in a cell compartment-specific manner. Through these studies, we hope to gain greater insight into TTP biology and the mechanism of ARE-dependent mRNA turnover.

Disclosures

The authors have no financial conflict of interest.

References

1. Beutler, B., and A. Cerami. 1989. The biology of cachectin/TNF—a primary mediator of the host response. *Annu. Rev. Immunol.* 7: 625–655.
2. Kontoyiannis, D., M. Pasparakis, T. T. Pizarro, F. Cominelli, and G. Kollias. 1999. Impaired on/off regulation of TNF biosynthesis in mice lacking TNF AU-rich elements: implications for joint and gut-associated immunopathologies. *Immunity* 10: 387–398.
3. Taylor, G. A., E. Carballo, D. M. Lee, W. S. Lai, M. J. Thompson, D. D. Patel, D. I. Schenkman, G. S. Gilkeson, H. E. Broxmeyer, B. F. Haynes, and P. J. Blackshear. 1996. A pathogenetic role for TNF-α in the syndrome of cachexia, arthritis, and autoimmunity resulting from tristetraprolin (TTP) deficiency. *Immunity* 4: 445–454.
4. Carballo, E., W. S. Lai, and P. J. Blackshear. 1998. Feedback inhibition of macrophage tumor necrosis factor-α production by tristetraprolin. *Science* 281: 1001–1005.
5. Lai, W. S., E. Carballo, J. R. Strum, E. A. Kennington, R. S. Phillips, and P. J. Blackshear. 1999. Evidence that tristetraprolin binds to AU-rich elements and promotes the deadenylation and destabilization of tumor necrosis factor-α mRNA. *Mol. Cell. Biol.* 19: 4311–4323.
6. Brooks, S. A., J. E. Connolly, and W. F. Rigby. 2004. The role of mRNA turnover in the regulation of tristetraprolin expression: evidence for an extracellular signal-regulated kinase-specific, AU-rich element-dependent, autoregulatory pathway. *J. Immunol.* 172: 7263–7271.
7. Tchen, C. R., M. Brook, J. Saklatvala, and A. R. Clark. 2004. The stability of tristetraprolin mRNA is regulated by mitogen-activated protein kinase p38 and by tristetraprolin itself. *J. Biol. Chem.* 279: 32393–32400.
8. Cao, H., F. Dzineku, and P. J. Blackshear. 2003. Expression and purification of recombinant tristetraprolin that can bind to tumor necrosis factor-α mRNA and serve as a substrate for mitogen-activated protein kinases. *Arch. Biochem. Biophys.* 412: 106–120.
9. Carballo, E., H. Cao, W. S. Lai, E. A. Kennington, D. Campbell, and P. J. Blackshear. 2001. Decreased sensitivity of tristetraprolin-deficient cells to p38 inhibitors suggests the involvement of tristetraprolin in the p38 signaling pathway. *J. Biol. Chem.* 276: 42580–42587.
10. Mahtani, K. R., M. Brook, J. L. Dean, G. Sully, J. Saklatvala, and A. R. Clark. 2001. Mitogen-activated protein kinase p38 controls the expression and post-translational modification of tristetraprolin, a regulator of tumor necrosis factor-α mRNA stability. *Mol. Cell. Biol.* 21: 6461–6469.
11. Kedersha, N., and P. Anderson. 2001. Stress granules: sites of mRNA triage that regulate mRNA stability and translatability. *Biochem. Soc. Trans.* 30: 963–969.
12. Piecyk, M., S. Wax, A. R. Beck, N. Kedersha, M. Gupta, B. Maritim, S. Chen, C. Gueydan, V. Kruys, M. Streuli, and P. Anderson. 2000. TIA-1 is a translational silencer that selectively regulates the expression of TNF-α. *EMBO J.* 19: 4154–4163.
13. Stoecklin, G., T. Stubbs, N. Kedersha, S. Wax, W. F. Rigby, T. K. Blackwell, and P. Anderson. 2004. MK2-induced tristetraprolin: 14-3-3 complexes prevent stress granule association and ARE-mRNA decay. *EMBO J.* 23: 1313–1324.
14. Chrestensen, C. A., M. J. Schroeder, J. Shabanowitz, D. F. Hunt, J. W. Pelo, M. T. Worthington, and T. W. Sturgill. 2004. MAPKAP kinase 2 phosphorylates

tristetraprolin on in vivo sites including Ser^{178}, a site required for 14-3-3 binding. *J. Biol. Chem.* 279: 10176–10184.
15. Bridges, D., and G. B. Moorhead. 2004. 14-3-3 proteins: a number of functions for a numbered protein. *Sci. STKE* 2004: re10.
16. Laroia, G., B. Sarkar, and R. J. Schneider. 2002. Ubiquitin-dependent mechanism regulates rapid turnover of AU-rich cytokine mRNAs. *Proc. Natl. Acad. Sci. USA* 99: 1842–1846.
17. Heximer, S. P., A. D. Cristillo, L. Russell, and D. R. Forsdyke. 1998. Expression and processing of G_0/G_1 switch gene 24 (G0S24/TIS11/TTP/NUP475) RNA in cultured human blood mononuclear cells. *DNA Cell Biol.* 17: 249–263.
18. Lai, W. S., M. J. Thompson, and P. J. Blackshear. 1998. Characteristics of the intron involvement in the mitogen-induced expression of Zfp-36. *J. Biol. Chem.* 273: 506–517.
19. Ford, L. P., J. Watson, J. D. Keene, and J. Wilusz. 1999. ELAV proteins stabilize deadenylated intermediates in a novel in vitro mRNA deadenylation/degradation system. *Genes Dev.* 13: 188–201.
20. Peng, S. S., C. Y. Chen, N. Xu, and A. B. Shyu. 1998. RNA stabilization by the AU-rich element binding protein, HuR, an ELAV protein. *EMBO J.* 17: 3461–3470.
21. Lai, W. S., E. A. Kennington, and P. J. Blackshear. 2003. Tristetraprolin and its family members can promote the cell-free deadenylation of AU-rich element-containing mRNAs by poly(A) ribonuclease. *Mol. Cell. Biol.* 23: 3798–3812.
22. Brooks, S. A., J. E. Connolly, R. J. Diegel, R. A. Fava, and W. F. Rigby. 2002. Analysis of the function, expression, and subcellular distribution of human tristetraprolin. *Arthritis Rheum.* 46: 1362–1370.
23. Altschul, S. F., W. Gish, W. Miller, E. W. Myers, and D. J. Lipman. 1990. Basic local alignment search tool. *J. Mol. Biol.* 215: 403–410.
24. Zhu, W., M. A. Brauchle, F. Di Padova, H. Gram, L. New, K. Ono, J. S. Downey, and J. Han. 2001. Gene suppression by tristetraprolin and release by the p38 pathway. *Am. J. Physiol.* 281: L499–L508.
25. Johnson, B. A., J. R. Stehn, M. B. Yaffe, and T. K. Blackwell. 2002. Cytoplasmic localization of tristetraprolin involves 14-3-3-dependent and -independent mechanisms. *J. Biol. Chem.* 277: 18029–18036.
26. Chen, C. Y., R. Gherzi, S. E. Ong, E. L. Chan, R. Raijmakers, G. J. Pruijn, G. Stoecklin, C. Moroni, M. Mann, and M. Karin. 2001. AU binding proteins recruit the exosome to degrade ARE-containing mRNAs. *Cell* 107: 451–464.
27. Hamilton, B. J., C. M. Burns, R. C. Nichols, and W. F. Rigby. 1997. Modulation of AUUUA response element binding by heterogeneous nuclear ribonucleoprotein A1 in human T lymphocytes: the roles of cytoplasmic location, transcription, and phosphorylation. *J. Biol. Chem.* 272: 28732–28741.
28. Lai, W. S., E. A. Kennington, and P. J. Blackshear. 2002. Interactions of CCCH zinc finger proteins with mRNA: non-binding tristetraprolin mutants exert an inhibitory effect on degradation of AU-rich element-containing mRNAs. *J. Biol. Chem.* 277: 9606–9613.
29. Laroia, G., R. Cuesta, G. Brewer, and R. J. Schneider. 1999. Control of mRNA decay by heat shock-ubiquitin-proteasome pathway. *Science* 284: 499–502.
30. Rechsteiner, M., and S. W. Rogers. 1996. PEST sequences and regulation by proteolysis. *Trends Biochem. Sci.* 21: 267–271.
31. Rogers, S., R. Wells, and M. Rechsteiner. 1986. Amino acid sequences common to rapidly degraded proteins: the PEST hypothesis. *Science* 234: 364–368.
32. Kotlyarov, A., and M. Gaestel. 2001. Is MK2 (mitogen-activated protein kinase-activated protein kinase 2) the key for understanding post-transcriptional regulation of gene expression? *Biochem. Soc. Trans.* 30: 959–963.
33. Kontoyiannis, D., A. Kotlyarov, E. Carballo, L. Alexopoulou, P. J. Blackshear, M. Gaestel, R. Davis, R. Flavell, and G. Kollias. 2001. Interleukin-10 targets p38 MAPK to modulate ARE-dependent TNF mRNA translation and limit intestinal pathology. *EMBO J.* 20: 3760–3770.
34. Nolan, R. D., and H. R. Arnstein. 1969. The dissociation of rabbit reticulocyte ribosomes with EDTA and the location of messenger ribonucleic acid. *Eur. J. Biochem.* 9: 445–450.
35. Lykke-Andersen, J., and E. Wagner. 2005. Recruitment and activation of mRNA decay enzymes by two ARE-mediated decay activation domains in the proteins TTP and BRF-1. *Genes Dev.* 19: 351–361.
36. Neininger, A., D. Kontoyiannis, A. Kotlyarov, R. Winzen, R. Eckert, H. D. Volk, H. Holtmann, G. Kollias, and M. Gaestel. 2002. MK2 targets AU-rich elements and regulates biosynthesis of tumor necrosis factor and interleukin-6 independently at different post-transcriptional levels. *J. Biol. Chem.* 277: 3065–3068.
37. Winzen, R., M. Kracht, B. Ritter, A. Wilhelm, C. Y. Chen, A. B. Shyu, M. Muller, M. Gaestel, K. Resch, and H. Holtmann. 1999. The p38 MAP kinase pathway signals for cytokine-induced mRNA stabilization via MAP kinase-activated protein kinase 2 and an AU-rich region-targeted mechanism. *EMBO J.* 18: 4969–4980.
38. Schmidlin, M., M. Lu, S. A. Leuenberger, G. Stoecklin, M. Mallaun, B. Gross, R. Gherzi, D. Hess, B. A. Hemmings, and C. Moroni. 2004. The ARE-dependent mRNA-destabilizing activity of BRF1 is regulated by protein kinase B. *EMBO J.* 23: 4760–4769.